Published for SISSA by Springer

Received: December 9, 2010
Accepted: February 10, 2011
Published: February 25, 2011

The vector form factor at the next-to-leading order in $1/N_C$: chiral couplings $\mathrm{L}_9(\mu)$ and $\mathrm{C}_{88}(\mu) - \mathrm{C}_{90}(\mu)$

Antonio Pich,[a] **Ignasi Rosell**[a,b] **and Juan José Sanz-Cillero**[c]

[a] *Departament de Física Teòrica, IFIC, Universitat de València - CSIC, Apt. Correus 22085, E-46071 València, Spain*

[b] *Departamento de Ciencias Físicas, Matemáticas y de la Computación, Universidad CEU Cardenal Herrera, c/ Sant Bartomeu 55, E-46115 Alfara del Patriarca, València, Spain*

[c] *Istituto Nazionale di Fisica Nucleare INFN, Sezione di Bari, Via Orabona 4, I-70126 Bary, Italy*

E-mail: Antonio.Pich@uv.es, rosell@uch.ceu.es, cillero@ifae.es

Abstract: Using the Resonance Chiral Theory Lagrangian, we perform a calculation of the vector form factor of the pion at the next-to-leading order (NLO) in the $1/N_C$ expansion. Imposing the correct QCD short-distance constraints, one fixes the amplitude in terms of the pion decay constant F and resonance masses. Its low momentum expansion determines then the corresponding $\mathcal{O}(p^4)$ and $\mathcal{O}(p^6)$ low-energy chiral couplings at NLO, keeping control of their renormalization scale dependence. At $\mu_0 = 0.77\,\mathrm{GeV}$, we obtain $L_9(\mu_0) = (7.9 \pm 0.4) \cdot 10^{-3}$ and $C_{88}(\mu_0) - C_{90}(\mu_0) = (-4.6 \pm 0.4) \cdot 10^{-5}$.

Keywords: 1/N Expansion, Chiral Lagrangians, QCD

ArXiv ePrint: 1011.5771

© SISSA 2011

doi:10.1007/JHEP02(2011)109

JHEP02(2011)109

Contents

1 Introduction **1**

2 The Lagrangian **3**

3 The vector form factor of the pion **5**

4 The chiral couplings $L_9(\mu)$ and $C_{88}(\mu) - C_{90}(\mu)$ **8**
- 4.1 The large-N_C limit 9
- 4.2 $L_9(\mu)$ and $C_{88}(\mu) - C_{90}(\mu)$ at NLO 9
- 4.3 Phenomenology 10

5 Conclusions **12**

A Dispersion relations and loop contribution **13**

B The spectral functions $\mathrm{Im}\,\mathcal{F}(s)|_{m_1,m_2}$ **14**

C Next-to-leading-order corrections $\mathcal{F}_{\mathrm{NLO}}(s)|_{m_1,m_2}$ **16**

D NLO contributions to $L_9(\mu)$ and $C_{88}(\mu) - C_{90}(\mu)$ **17**

E Description in terms of Feynman diagrams **19**

1 Introduction

Effective field theories (EFT) are nowadays the standard tool to investigate the low-energy dynamics of Quantum Chromodynamics (QCD). In particular, the chiral symmetry is a crucial ingredient for the understanding of the light quark interactions. The dynamics of the pseudo-Goldstone bosons from the spontaneous symmetry breaking is provided by the corresponding EFT, Chiral Perturbation Theory (χPT), with a perturbative expansion in powers of light quark masses and external momenta [1–4]. This allows a systematic description of the long-distance regime of QCD, at energies below the lightest resonance mass. The precision required in present phenomenological applications makes necessary to include corrections of $\mathcal{O}(p^6)$. While many two-loop χPT calculations have been already carried out [5, 6], the large number of unknown low-energy constants (LECs) appearing at this order puts a clear limit to the achievable accuracy. The determination of these χPT couplings is compulsory to achieve further progress in our understanding of strong interactions at low energies.

In the resonance region, $E \sim M_R$, the chiral counting breaks down and the new heavier degrees of freedom — the resonances — have to be explicitly incorporated into

JHEP02(2011)109

the theory. A suitable alternative is then provided by the $1/N_C$ expansion in the limit of a large number of colours, $N_C \to \infty$ [7–13]. Assuming confinement, the strong dynamics is given at large N_C by tree-level diagrams with an infinite number of possible hadronic exchanges. This corresponds to the tree approximation of some local Lagrangian, being meson loops suppressed by higher powers of $1/N_C$ [7–9]. Resonance Chiral Theory (RχT) provides an appropriate framework to incorporate these massive mesonic states within a chiral invariant phenomenological Lagrangian [14–16]. The operators of the RχT action are constructed such that they remain unchanged under flavour transformations $\mathrm{U}(3)_L \otimes \mathrm{U}(3)_R$. After integrating out the heavy fields, the χPT Lagrangian is recovered at low energies with explicit values of the chiral LECs in terms of resonance parameters. The short-distance properties of QCD impose stringent constraints on the RχT couplings and provide important information for the extraction of the low-energy χPT parameters. The amplitudes are thus enforced to follow the known high-energy QCD behaviour, introducing in the long-distance description important information from the underlying theory [10–13].

Clearly, we cannot determine at present the infinite number of meson couplings which characterize the large-N_C Lagrangian. However, one can perform useful approximations in terms of a finite number of meson fields. Truncating the infinite tower of mesons to the lowest resonances with 0^{-+}, 0^{++}, 1^{--} and 1^{++} quantum numbers, one gets a very successful prediction for the $\mathcal{O}(p^4)$ χPT couplings at large N_C [13]. Already at this level the comparison with experimental determinations of the $\mathcal{O}(p^4)$ chiral couplings shows a remarkable agreement. Some $\mathcal{O}(p^6)$ LECs have been also estimated in this way, by studying appropriate sets of Green functions (see ref. [16] and references therein). All the required terms in the RχT Lagrangian that may contribute to the $\mathcal{O}(p^6)$ LECs at LO in $1/N_C$ were classified in ref. [16].

Since chiral loop corrections are of next-to-leading order (NLO) in the $1/N_C$ expansion, the large-N_C determination of the LECs is unable to control their renormalization-scale dependence. First analyses of resonance loop contributions to the running of $L_{10}(\mu)$ and $L_9(\mu)$ were attempted in refs. [17] and [18], respectively. In spite of all the complexity associated with the still not so well understood renormalization of RχT [18–25], these pioneering calculations showed the potential predictability at the NLO in $1/N_C$.

Using dispersion relations we can avoid the technicalities associated with the renormalization procedure [24, 26, 27]. This allows one to understand the underlying physics in a much more transparent way. Still, a fully equivalent diagrammatic calculation is possible, although the derivation and presentation is slightly more cumbersome [17, 18, 28]. In particular, the subtle cancellations among many unknown renormalized couplings found in ref. [18] and the relative simplicity of the final result can be better understood in terms of the imposed short-distance constraints within the dispersive approach. Following these ideas we determined, up to NLO in $1/N_C$, the couplings $L_8(\mu)$ and $C_{38}(\mu)$ in ref. [26] and $L_{10}(\mu)$ and $C_{87}(\mu)$ in ref. [27]. In this article we present the study of the vector form factor (VFF) of the pion, which allows us to estimate the χPT coupling $L_9(\mu)$ and the $\mathcal{O}(p^6)$ combination $C_{88}(\mu) - C_{90}(\mu)$ up to NLO in $1/N_C$.

In order to establish the notation, the RχT Lagrangian is introduced in the next section. The analysis of the VFF in the resonance region is performed in section 3, while

JHEP02(2011)109

section 4 contains the determination of $L_9(\mu)$ and $C_{88}(\mu) - C_{90}(\mu)$. A summary of our results is finally given in section 5. In order to ease the reading of the text, we have shifted the technical details on the calculation of the spectral function, the full VFF and the chiral coupling expressions to the appendices.

2 The Lagrangian

We will adopt the Single Resonance Approximation (SRA), where just the lightest resonances with non-exotic quantum numbers are considered.[1] On account of the large-N_C limit, the mesons are put together into U(3) multiplets. Hence, our degrees of freedom are the pseudo-Goldstone bosons (the lightest pseudoscalar mesons) along with massive multiplets of the type $V(1^{--})$, $A(1^{++})$, $S(0^{++})$ and $P(0^{-+})$. With them, we construct the most general action that preserves chiral symmetry. Since we are interested in determining the χPT low-energy constants and the study of the short-distance behaviour, the chiral limit will be taken all along the paper. No information is lost as the chiral LECs are independent of the light quark masses.

Resonance Chiral Theory must satisfy the high-energy behaviour dictated by QCD. To comply with this requirement we will only consider operators constructed with chiral tensors of $\mathcal{O}(p^2)$; interactions with higher-order chiral tensors tend to violate the asymptotic short-distance behaviour prescribed by QCD [13, 22, 23]. Likewise, it has been shown in some cases that resonance operators with higher number of derivatives can be simplified into terms with less derivatives, terms without resonances and operators that contribute to other hadronic amplitudes, by means of the equations of motion and convenient meson field redefinitions [14, 16, 18–21, 28].

The different terms in the Lagrangian can be classified by their number of resonance fields:

$$\mathcal{L}_{R\chi T} = \mathcal{L}_G + \sum_{R_1} \mathcal{L}_{R_1} + \sum_{R_1,R_2} \mathcal{L}_{R_1 R_2} + \dots , \tag{2.1}$$

where the dots denote operators with three or more resonance fields, and the indices R_i run over all different resonance multiplets, V, A, S and P. The term with only pseudo-Goldstone bosons is given by [2–4]

$$\mathcal{L}_G = \frac{F^2}{4} \langle\, u_\mu u^\mu + \chi_+ \,\rangle \,. \tag{2.2}$$

[1] In ref. [29–31], it has been argued that large discrepancies may occur between the values of the masses and couplings of the full large-N_C theory and those from descriptions with a finite number of resonances. Even in this case, it is found that one can obtain safe determinations of the LECs as far as one is able to construct a good interpolator that reproduces the right asymptotic behaviour at low and high energies. Further issues related to the truncation of the spectrum to a finite number of resonances are discussed in ref. [32–34].

JHEP02(2011)109

The second term in eq. (2.1) corresponds to the operators with one massive resonance [14],

$$\begin{aligned}
\mathcal{L}_V &= \frac{F_V}{2\sqrt{2}}\langle\, V_{\mu\nu} f_+^{\mu\nu}\,\rangle + \frac{i\,G_V}{2\sqrt{2}}\langle\, V_{\mu\nu}[u^\mu, u^\nu]\,\rangle\,,\\
\mathcal{L}_A &= \frac{F_A}{2\sqrt{2}}\langle\, A_{\mu\nu} f_-^{\mu\nu}\,\rangle\,,\\
\mathcal{L}_S &= c_d\langle\, S u_\mu u^\mu\,\rangle + c_m\langle\, S\chi_+\,\rangle\,,\\
\mathcal{L}_P &= i\,d_m\langle\, P\chi_-\,\rangle\,.
\end{aligned} \tag{2.3}$$

The Lagrangian $\mathcal{L}_{R_1R_2}$ contains the kinetic resonance terms and the remaining operators with two resonance fields [14, 16, 18]. We show only the terms that contribute to the vector form factor of the pion, taking into account that here we just consider the lowest-mass two-particle absorptive channels, with two pseudo-Goldstone bosons or one pseudo-Goldstone and one resonance. In the energy range we are interested in, exchanges of two heavy resonances are kinematically suppressed. Hence, the relevant operators are

$$\begin{aligned}
\Delta\mathcal{L}_{SA} &= \lambda_1^{SA}\langle\, \{\nabla_\mu S, A^{\mu\nu}\} u_\nu\,\rangle\,,\\
\Delta\mathcal{L}_{SP} &= \lambda_1^{SP}\langle\, u_\alpha\{\nabla^\alpha S, P\}\,\rangle\,,\\
\Delta\mathcal{L}_{PV} &= i\lambda_1^{PV}\langle\, [\nabla^\mu P, V_{\mu\nu}]u^\nu\,\rangle\,,\\
\Delta\mathcal{L}_{VA} &= i\lambda_2^{VA}\langle\, [V^{\mu\nu}, A_{\nu\alpha}]h_\mu^\alpha\,\rangle + i\lambda_3^{VA}\langle\, [\nabla^\mu V_{\mu\nu}, A^{\nu\alpha}]u_\alpha\,\rangle\\
&\quad + i\lambda_4^{VA}\langle\, [\nabla_\alpha V_{\mu\nu}, A^{\alpha\nu}]u^\mu\,\rangle + i\lambda_5^{VA}\langle\, [\nabla_\alpha V_{\mu\nu}, A^{\mu\nu}]u^\alpha\,\rangle\,.
\end{aligned} \tag{2.4}$$

All coupling constants are real, the brackets $\langle\ldots\rangle$ denote a trace of the corresponding flavour matrices, and the standard definitions for the u^μ, $\chi_\pm$, $f_\pm^{\mu\nu}$ and $h^{\mu\nu}$ chiral tensors of pseudo-Goldstones are provided in refs. [14, 16].

Our Lagrangian $\mathcal{L}_{R\chi T}$ satisfies the N_C counting rules for a theory with U(3) multiplets. Therefore, only operators that have one trace in the flavour space are considered. Note that local terms with two traces in flavour space, which are of NLO in $1/N_C$, cannot contribute at tree-level to the VFF because the final two-pion state has isospin $I = 1$. The different fields, masses and momenta are of $\mathcal{O}(N_C^0)$ in the $1/N_C$ expansion. Taking into account the interaction terms, one can check that F, F_V, G_V, F_A, c_d, c_m and d_m are $\mathcal{O}(\sqrt{N_C})$ and the $\lambda_i^{R_1R_2}$ are $\mathcal{O}(N_C^0)$. The mass dimension of these parameters is $[F] = [F_V] = [G_V] = [F_A] = [c_d] = [c_m] = [d_m] = E$ and $[\lambda_i^{R_1R_2}] = E^0$.

Note that the U(3) equations of motion have been used in order to reduce the number of operators. For instance, terms like $\langle P\,\nabla_\mu u^\mu\rangle$ are not present in eq. (2.3), since they can be transformed into operators that, either have been already considered, or contain a higher number of mesons by means of the equations of motion and convenient meson field redefinitions [14].

The RχT Lagrangian (2.1) contains a large number of unknown coupling constants. However, as we will see in the next section, the short-distance QCD constraints allow us to determine many of them. In the observable at hand and with our assumptions, we initially have ten couplings or combinations of them (F, F_V, G_V, F_A, c_d, λ_1^{SA}, λ_1^{SP}, λ_1^{PV}, $-2\lambda_2^{\rm VA} + \lambda_3^{\rm VA}$ and $2\lambda_2^{\rm VA} - 2\lambda_3^{\rm VA} + \lambda_4^{\rm VA} + 2\lambda_5^{\rm VA}$) and four resonance masses (M_V, M_A, M_S

JHEP02(2011)109

and M_P). As we will see in section 3, after imposing a good short-distance behaviour of this observable, the number of parameters reduces to three couplings (F, G_V and F_A) and three masses (M_V, M_A and M_S). The Weinberg sum-rules associated with the left-right correlator [35, 36] allow us to further reduce the number of inputs; the amplitude is finally determined in terms of just F and the three masses M_V, M_A and M_S. The role of the information coming from the underlying theory is thus fundamental.

3 The vector form factor of the pion

Our observable is defined through the two pseudo-Goldstone matrix element of the vector current:

$$\langle\, \pi^+(p_1)\, \pi^-(p_2)\, |\, \frac{1}{2}\left(\bar{u}\gamma^\mu u - \bar{d}\gamma^\mu d\right) |0\,\rangle = \mathcal{F}(s)\,(p_1 - p_2)^\mu, \tag{3.1}$$

where $s \equiv (p_1 + p_2)^2$. At very low energies, $\mathcal{F}(s)$ has been studied within the χPT framework up to $\mathcal{O}(p^6)$ [2–4, 37, 38]. RχT and the $1/N_C$ expansion have also been used to determine $\mathcal{F}(s)$ at the ρ meson peak, including appropriate resummations of subleading logarithms from two pseudo-Goldstone channels [39–45]. A first systematic study of the VFF at NLO in $1/N_C$ was performed in ref. [18]. Although the general structure was well established there, the present article answers and solves three important questions raised in that previous paper:

- In ref. [18] only operators with at most one resonance field were included (except for the kinetic resonance terms) [14]. However, as suggested in the appendix C of that article, this assumption is not really justified and leads to problems with the asymptotic short distance behaviour. In the present paper, we have considered all the operators needed to describe the absorptive cuts with two chiral pseudo-Goldstones and those with one pseudo-Goldstone and one resonance, being higher thresholds with two resonances highly suppressed in the energy region that we consider [27].

- Due to this first issue, in ref. [18] the logarithmic part of $\mathcal{F}(s)$ was badly behaved at high energies. It was not possible to enforce a vanishing form factor at $s \to \infty$ without the inclusion of new hadronic operators in the leading Lagrangian. The inclusion of those terms in the present article will allow us to recover the expected high-energy dependence for the VFF in QCD [46, 47].

- The final result of ref. [18] contained the unknown RχT couplings $\widetilde{L}_9$ and $\widetilde{C}_{88} - \widetilde{C}_{90}$, which are the analogous ones to the χPT LECs L_9 and $C_{88} - C_{90}$. In the present work, they are fully determined by means of the high-energy matching with QCD [22, 23].

Within Resonance Chiral Theory the diagrams contributing to the VFF at leading order in $1/N_C$ are shown in figure 1. They generate the result

$$\mathcal{F}_{R\chi T}(s) = 1 + \frac{F_V G_V}{F^2}\frac{s}{M_V^2 - s}\,. \tag{3.2}$$

JHEP02(2011)109

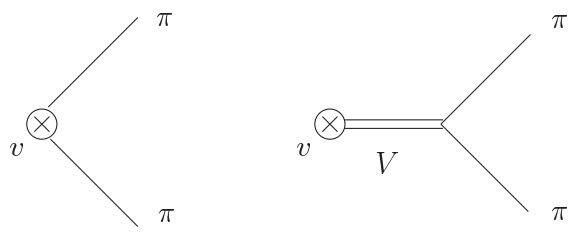

Figure 1. Tree-level contributions to the vector form factor of the pion. A single line stands for a pseudo-Goldstone boson while a double line indicates a resonance.

Considering that the form factor is constrained to be zero at infinite momentum transfer [46, 47], the vector couplings should satisfy

$$F_V G_V = F^2 \,, \tag{3.3}$$

which implies

$$\mathcal{F}_{R\chi T}\,(s) = \frac{M_V^2}{M_V^2 - s}\,. \tag{3.4}$$

The subleading corrections can be calculated by means of dispersive relations. Once the one-loop absorptive parts of $\mathcal{F}_{R\chi T}\,(s)$ are known, one can reconstruct the full form factor up to appropriate subtraction terms. We can separate then the leading and subleading parts of the amplitude in the form

$$\mathcal{F}_{R\chi T}\,(s) = \frac{M_V^2}{M_V^2 - s} + \mathcal{F}(s)_{\text{NLO}}\,, \tag{3.5}$$

with $\mathcal{F}(s)^{\text{NLO}}$ containing the one-loop contribution (figure 2) and the subleading part δ_{NLO} of the resonance coupling combination $F_V G_V/F^2 = 1 + \delta_{\text{NLO}}$ (for details see appendix E):

$$\mathcal{F}(s)_{\text{NLO}} = \delta_{\text{NLO}} \frac{s}{M_V^2 - s} + \mathcal{F}^{1\ell}(s)\,. \tag{3.6}$$

The explicit form for the subtracted one-loop amplitude $\mathcal{F}^{1\ell}(s)$ can be found in appendices A and C, being fully determined by the spectral function $\text{Im}\mathcal{F}(s)$ through a once-subtracted dispersion relation. It vanishes at $s = 0$ and has no contribution to the real part of the pole at $s = M_V^2$. The subleading correction to the couplings, δ_{NLO}, is fixed by means of the high-energy matching after demanding that it cancels the bad behaviour of $\mathcal{F}^{1\ell}(s) = \delta_{\text{NLO}} + \mathcal{O}(s^{-1})$ when $s \to \infty$. Furthermore, the NLO term $\mathcal{F}(s)_{\text{NLO}}$ can be neatly separated into its different contributions from the various two-meson absorptive channels $\mathcal{F}(s)_{\text{NLO}}|_{m_1,m_2}$, given by the corresponding $\mathcal{F}^{1\ell}(s)|_{m_1,m_2}$ and the consequent $\delta_{\text{NLO}}|_{m_1,m_2}$. These details are relegated to appendices B and C.

Although in this article we follow the procedure of refs. [26, 27], our results can be also derived in an utterly equivalent way through a Feynman diagram computation and the standard renormalization procedure. This derivation is slightly more complex and its detailed explaination is relegated to appendix E.

JHEP02(2011)109

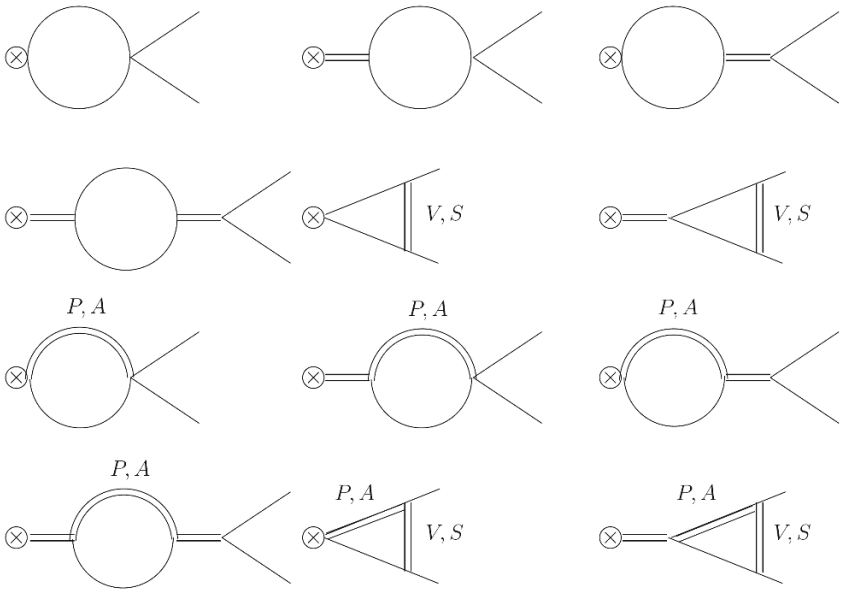

Figure 2. One-loop contributions to the vector form factor of the pion with absorptive cut. A single line stands for a pseudo-Goldstone boson while a double line indicates a resonance.

We will consider only the effects of absorptive loops with two pseudo-Goldstones ($\pi\pi$) or with one pseudo-Goldstone and a resonance ($R\pi$). Two-resonance channels RR' have their thresholds at $(M_R + M_R')^2 \gtrsim 2\,\mathrm{GeV}^2$ and their impact on the LEC determination is expected to be negligible [27]. Taking this into account, we extract our RχT form factor through the following short-distance matching procedure:

1. Determine the spectral function of the considered absorptive cuts ($\pi\pi$ and $R\pi$). The full expressions are shown in eqs. (B.1), (B.2) and (B.3) of appendix B.

2. We demand $\mathrm{Im}\mathcal{F}(s)$ to be well-behaved at high energies, i.e., it must vanish when $s \to \infty$. In the present work, we will actually impose this constraint channel by channel, i.e., we will demand that each separate two-meson cut $\mathrm{Im}\mathcal{F}(s)|_{m_1,m_2}$ vanishes at $s \to \infty$. For spin-0 mesons this must be so as its one-loop contribution to the spectral function is essentially its VFF at LO (which vanishes at infinite momentum) times the partial-wave scattering amplitude at LO (which is upper bounded). For higher spin resonances the derivation is more cumbersome as the Lorentz structure allows for the proliferation of form factors and the unitarity relations are not that simple. Still, in many situations it has been already found that amplitudes with massive spin-1 mesons as final states must go to zero at high energies even faster, due to the presence of extra powers of momenta in the unitarity relations coming from intermediate longitudinal polarizations [27]. In summary, we will assume $\mathrm{Im}\mathcal{F}(s)|_{m_1,m_2} \to 0$ when $s \to \infty$ for every absorptive two-meson cut under consideration, regardless of the spin of the intermediate mesons.

   In the case of the $\pi\pi$ cut we have found two constraints, which are consistent with the literature,

$$F_V G_V = F^2\,, \qquad 3\,G_V^2 + 2\,c_d^2 = F^2\,, \tag{3.7}$$

JHEP02(2011)109

where the first one coincides with eq. (3.3), that is, with the constraint obtained with the vector form factor at leading-order [15]. The second one was derived in ref. [48] from the LO $\pi\pi$ scattering amplitude. It is interesting to remark that the $c_d = 0$ limit of this second relation, $G_V = F/\sqrt{3}$, has been obtained recently from a study of $\tau^- \to P^- \gamma \nu_\tau$ decays ($P = \pi, K$) [49]. We have used these constraints to fix F_V and c_d^2.

For the $P\pi$ cut, the only possible solution is to kill the whole contribution by means of

$$\lambda_1^{\rm PV} = 0\,, \tag{3.8}$$

which is consistent with the large-N_C constraint from the vector form factor into $P\pi$, studied in ref. [27].

The analysis of the $A\pi$ cut leads to more than one real solution. We have chosen the solutions consistent with previous works [24, 27], where the NLO contributions in $1/N_C$ to the $\Pi_{VV}(s)$ correlator coming from tree-level form factors to resonance fields were studied:

$$\begin{aligned} -2\lambda_2^{\rm VA} + \lambda_3^{\rm VA} = 0\,, \qquad -\lambda_3^{\rm VA} + \lambda_4^{\rm VA} + 2\lambda_5^{\rm VA} = \frac{F_A}{F_V}\,, \\ \lambda_1^{\rm SA} = -\frac{F_A\, G_V\, \left(M_A^2 - 4\, M_V^2\right)}{3\sqrt{2} M_A^2 c_d\, F_V}\,. \end{aligned} \tag{3.9}$$

The first two constraints, in the first line, come from the analysis of the $A\pi$ vector form-factor. The last relation with λ_1^{SA} is then needed to make $\mathrm{Im}\mathcal{F}(s)|_{A\pi} \to 0$ for $s \to \infty$.

After imposing the relations (3.7), (3.8) and (3.9) the spectral functions can be expressed in terms of G_V, F_A, F and masses, as shown in eqs. (B.6), (B.7) and (B.8).

3. The spectral function is now ready for the once-subtracted dispersion relation provided in the appendix A in eq. (A.4), which allows to reconstruct the full form factor up to the pole position at $s = M_V^2$ and the real part of its residue.

4. Finally, we impose that the whole $\mathcal{F}_{R\chi T}(s)$ vanishes at short distances — not only its imaginary part —. This fixes the real part of the residue at $s = M_V^2$ and, consequently, the NLO correction $\delta_{\rm NLO}$ in eq. (3.6). In order to ease the reading of the manuscript, the complicated expressions for the well-behaved contributions to the different channels are provided in appendix C, in eqs. (C.1), (C.2) and (C.3).

4 The chiral couplings $L_9(\mu)$ and $C_{88}(\mu) - C_{90}(\mu)$

The low-momentum expansion of $\mathcal{F}(s)$ is determined by χPT [2–4, 37, 38]. The corresponding expression in the chiral limit reads

$$\begin{aligned} \mathcal{F}_{\chi PT}(s) = 1 + \frac{2\,s}{F^2}\left\{L_9(\mu) + \frac{\Gamma_9}{32\pi^2}\left(\frac{5}{3} - \log\frac{-s}{\mu^2}\right)\right\} \\ -\frac{4\,s^2}{F^4}\left\{C_{88}(\mu) - C_{90}(\mu) - \frac{\Gamma_{88}^{(L)} - \Gamma_{90}^{(L)}}{32\pi^2}\left(\frac{5}{3} - \log\frac{-s}{\mu^2}\right) + \mathcal{O}\left(N_C^0\right)\right\} + \mathcal{O}\left(s^3\right)\,, \end{aligned} \tag{4.1}$$

JHEP02(2011)109

with [2–6]

$$\Gamma_9 = \frac{1}{4}\,, \qquad \Gamma_{88}^{(L)} - \Gamma_{90}^{(L)} = -\frac{2L_1}{3} + \frac{L_2}{3} - \frac{L_3}{2} + \frac{L_9}{4}\,. \tag{4.2}$$

The couplings F^2, L_9, C_{88}/F^2 and C_{90}/F^2 are of $\mathcal{O}(N_C)$, while Γ_9, $\Gamma_{88}^{(L)}/F^2$ and $\Gamma_{90}^{(L)}/F^2$ are of $\mathcal{O}(N_C^0)$ and represent a NLO effect.

The low-energy expansion of eqs. (3.4) and (3.5), obtained, respectively, within Resonance Chiral Theory at leading-order and at next-to-leading order in the $1/N_C$ expansion, allows to determine the chiral couplings L_9 and $C_{88} - C_{90}$ at LO and at NLO.

4.1 The large-N_C limit

At leading-order in $1/N_C$, eq. (4.1) becomes

$$\mathcal{F}_{\chi PT}(s) = 1 + \frac{2\,s}{F^2}\left\{L_9 + \mathcal{O}\big(N_C^0\big)\right\} - \frac{4\,s^2}{F^4}\left\{C_{88} - C_{90} + \mathcal{O}(N_C)\right\} + \mathcal{O}\big(s^3\big)\,. \tag{4.3}$$

Within RχT in the large-N_C limit, eq. (3.4) can be now expanded at low energies:

$$\mathcal{F}_{R\chi T}(s) = \frac{M_V^2}{M_V^2 - s} = 1 + \frac{s}{M_V^2} + \frac{s^2}{M_V^4} + \mathcal{O}\big(s^3\big)\,. \tag{4.4}$$

The matching between (4.3) and (4.4) fixes L_9 and $C_{88} - C_{90}$ at LO [15, 16],

$$L_9 = \frac{F^2}{2M_V^2}\,, \qquad C_{88} - C_{90} = -\frac{F^4}{4M_V^4}\,. \tag{4.5}$$

4.2 $L_9(\mu)$ and $C_{88}(\mu) - C_{90}(\mu)$ at NLO

Following the same steps as before, let us determine the related $\mathcal{O}(p^4)$ and $\mathcal{O}(p^6)$ low-energy constants by matching eq. (4.1) and the low-energy expansion of eq. (3.5),

$$\begin{aligned}\mathcal{F}_{R\chi T}(s) = 1 &+ \frac{2s}{F^2}\left\{\frac{F^2}{2M_V^2} + \bar{\xi}^{(2)} + \frac{\Gamma_9}{32\pi^2}\left(\frac{5}{3} - \log\frac{-s}{M_V^2}\right)\right\} \\ &- \frac{4\,s^2}{F^4}\left\{-\frac{F^4}{4M_V^4} + \bar{\xi}^{(4)} - \frac{\Gamma_{88}^{(L)} - \Gamma_{90}^{(L)}}{32\pi^2}\left(\frac{5}{3} - \log\frac{-s}{M_V^2}\right)\right\} + \mathcal{O}\big(s^3\big)\,,\end{aligned} \tag{4.6}$$

where the $\bar{\xi}^{(2n)}$ are the relevant $\mathcal{O}(s^n)$ coefficients of the low-energy expansion of $\mathcal{F}_{\rm NLO}(s)$, once the structure coming from the χPT one-loop diagram has been subtracted from the $\pi\pi$ channel. The separated contributions $\bar{\xi}^{(2n)}_{m_1,m_2}$ from each absorptive two-meson cut $\mathcal{F}_{NLO}(s)|_{m_1,m_2}$ are provided in appendix D, being each of them independent of the renormalization scale μ.

By comparing the χPT expression (4.1) to the RχT low-energy expansion (4.6), it is straightforward to estimate the chiral LECs $L_9(\mu)$ and $C_{88}(\mu) - C_{90}(\mu)$ up to NLO in $1/N_C$:

$$\begin{aligned} L_9(\mu) &= \frac{F^2}{2M_V^2} + \bar{\xi}^{(2)} + \frac{\Gamma_9}{32\pi^2}\,\ln\frac{M_V^2}{\mu^2}\,, \\ C_{88}(\mu) - C_{90}(\mu) &= -\frac{F^4}{4M_V^2} + \bar{\xi}^{(4)} - \frac{\Gamma_{88}^{(L)} - \Gamma_{90}^{(L)}}{32\pi^2}\,\ln\frac{M_V^2}{\mu^2}\,, \end{aligned} \tag{4.7}$$

JHEP02(2011)109

where

$$\Gamma_{88}^{(L)} - \Gamma_{90}^{(L)} = \frac{3G_V^2}{8M_V^2} - \frac{c_d^2}{4M_S^2} + \frac{F_V G_V}{8M_V^2} = \frac{F^2 - 3G_V^2}{8M_S^2} - \frac{F^2 + 3G_V^2}{8M_V^2} \tag{4.8}$$

matches the corresponding $\mathcal{O}(p^6)$ running at NLO in $1/N_C$. Note that the large-N_C relations $L_2 = 2L_1 = \frac{G_V^2}{4M_V^2}$, $L_3 = -\frac{3G_V^2}{4M_V^2} + \frac{c_d^2}{2M_S^2}$ and $L_9 = \frac{F_V G_V}{2M_V^2}$ [14] have been used in eq. (4.2). The high-energy constraints $F_V G_V = F^2$ and $2c_d^2 = F^2 - 3G_V^2$ of eq. (3.7) have been employed to obtain the result on the r.h.s. of eq. (4.8).

4.3 Phenomenology

Using $M_V \simeq 0.77\,\text{GeV}$ and $F \simeq 89\,\text{MeV}$, one gets the large-N_C estimates from eq. (4.5): $L_9 \simeq 6.7 \cdot 10^{-3}$ and $C_{88} - C_{90} \simeq -4.5 \cdot 10^{-5}$. At $\mu_0 = 770\,\text{MeV}$, the phenomenological determinations $L_9(\mu_0) = (6.9 \pm 0.7) \cdot 10^{-3}$ [2–4, 13] and $L_9(\mu_0) = (5.93 \pm 0.43) \cdot 10^{-3}, C_{88}(\mu_0) - C_{90}(\mu_0) = (-5.5 \pm 0.5) \cdot 10^{-5}$ [37, 38], obtained respectively from an $\mathcal{O}(p^4)$ and an $\mathcal{O}(p^6)$ ChPT fit, agree approximately with the LO estimates.

Large-N_C estimates are naively expected to approximate well the couplings at scales of the order of the relevant dynamics involved ($\mu \sim M_R$). However, they always carry an implicit error because of the uncertainty on μ. This theoretical uncertainty is rather important in couplings generated through scalar meson exchange, such as $L_8(\mu)$. In the present case, it also has a moderate importance. The size of the NLO corrections in $1/N_C$ to $L_9(\mu)$ and $C_{88}(\mu) - C_{90}(\mu)$ can be estimated by regarding their variations with μ. These are respectively given by

$$\frac{\partial L_9(\mu)}{\partial \log \mu^2} = -\frac{\Gamma_9}{32\pi^2} = -0.8 \cdot 10^{-3}, \qquad \frac{\partial \left(C_{88}(\mu) - C_{90}(\mu)\right)}{\partial \log \mu^2} = \frac{\Gamma_{88}^{(L)} - \Gamma_{90}^{(L)}}{32\pi^2} \simeq 0.9 \cdot 10^{-5}. \tag{4.9}$$

So far, we have been working within a $\text{U}(3)_L \otimes \text{U}(3)_R$ framework, but we are actually interested on the couplings of the standard $\text{SU}(3)_L \otimes \text{SU}(3)_R$ chiral theory. Thus, a matching between the two versions of χPT must be performed. Nonetheless, on the contrary to what happens with other matrix elements (e.g. the $S - P$ correlator [26]), the spin-1 two-point functions do not gain contributions from the U(3)-singlet chiral pseudo-Goldstone; the η_1 does neither enter at tree-level nor in the one-loop correlators. Therefore, the corresponding LECs are identical in both theories at leading and next-to-leading order in $1/N_C$: $L_9(\mu)^{\text{U}(3)} = L_9(\mu)^{\text{SU}(3)}$, $(C_{88}(\mu) - C_{90}(\mu))^{\text{U}(3)} = (C_{88}(\mu) - C_{90}(\mu))^{\text{SU}(3)}$.

The needed input parameters are defined in the chiral limit. We take the ranges [2–4, 50] $M_V = (770 \pm 5)\,\text{MeV}$, $M_S = (1090 \pm 110)\,\text{MeV}$ and $F = (89 \pm 2)\,\text{MeV}$. The resonance couplings G_V and F_A can be fixed in terms of F and masses if one considers the short-distance conditions obeyed by the left-right correlator [13]. The constraint of eq. (3.3), coming from the vector form factor of the pion, and those from the first and second Weinberg sum rules [35, 36] determine the vector and axial-vector couplings at LO in $1/N_C$ [24, 27],

$$F_V^2 = F^2 \frac{M_A^2}{M_A^2 - M_V^2}, \qquad G_V^2 = F^2 \frac{M_A^2 - M_V^2}{M_A^2}, \qquad F_A^2 = F^2 \frac{M_V^2}{M_A^2 - M_V^2}, \tag{4.10}$$

JHEP02(2011)109

	1st Approach	2nd Approach
$10^3 \cdot L_9$ at LO	6.68	6.68
$10^3 \cdot \bar{\xi}^{(2)}_{\pi\pi}$	0.11	−0.04
$10^3 \cdot \bar{\xi}^{(2)}_{P\pi}$	0.00	0.00
$10^3 \cdot \bar{\xi}^{(2)}_{A\pi}$	1.12	1.00
$10^5 \cdot (C_{88} - C_{90})$ at LO	−4.46	−4.46
$10^5 \cdot \bar{\xi}^{(4)}_{\pi\pi}$	0.76	0.71
$10^5 \cdot \bar{\xi}^{(4)}_{P\pi}$	0.00	0.00
$10^5 \cdot \bar{\xi}^{(4)}_{A\pi}$	−0.88	−0.73

Table 1. Different contributions to the chiral couplings within the two numerical approaches explained in the text.

with $M_A > M_V$. Due to the large width of the $a_1(1260)$ meson, the determination of the Lagrangian parameter M_A is far from trivial. From the observed rates $\Gamma(\rho^0 \to e^+e^-) = (7.02 \pm 0.13)$ keV [50] and $\Gamma\,(a_1 \to \pi\gamma) = (650 \pm 250)$ keV [50], and considering (4.10), one finds $M_A = (938 \pm 13)$ MeV and $M_A = (960 \pm 80)$ MeV. Another large-N_C determination of M_A was obtained in ref. [51] from the study of the $\pi \to e\nu_e\gamma$ decay, which yields $M_A = (998 \pm 49)$ MeV. We cannot use the information coming from $\Gamma(\rho \to 2\pi) = (149.4 \pm 1.0)$ MeV [50] in order to determine M_A, since G_V is constrained by eq. (3.7) to be smaller than $F/\sqrt{3}$, which results in $M_A < 940$ MeV. In spite of the dispersion of values for M_A, one gets a consistent description in the range $M_A = (920 \pm 20)$ MeV, which we will take as our input. The resulting numerical predictions for the LECs are

$$\begin{aligned} L_9(\mu_0) &= (7.9 \pm 0.4) \cdot 10^{-3}, \\ C_{88}(\mu_0) - C_{90}(\mu_0) &= (-4.6 \pm 0.4) \cdot 10^{-5}, \end{aligned} \tag{4.11}$$

being μ_0 the usual renormalization scale, $\mu_0 = 770$ MeV.

Alternatively, one could also use the phenomenological values for G_V, F_A and the axial-vector mass, instead of fixing them through the Weinberg sum-rules. Thus, one may employ $M_A = (1200 \pm 200)$ MeV [50], and $F_A = (120 \pm 20)$ MeV, from the observed rate $\Gamma\,(a_1 \to \pi\gamma) = (650 \pm 250)$ keV [50]. The constraint of eq. (3.7) implies that $G_V < F/\sqrt{3}$, so that we take the range $G_V \in [40, 50]$ MeV. For the remaining inputs M_V, M_S and F, we consider the same values used before, yielding the predictions

$$\begin{aligned} L_9(\mu_0) &= (7.6 \pm 0.6) \cdot 10^{-3}, \\ C_{88}(\mu_0) - C_{90}(\mu_0) &= (-4.5 \pm 0.5) \cdot 10^{-5}. \end{aligned} \tag{4.12}$$

As it can be observed, the influence of using the first or the second approach is not crucial at the present level of accuracy. We take the values in (4.11), which include more theoretical constraints, as our final next-to-leading-order estimates for the LECs.

In table 1 we present the different contributions to the LECs within the first and second approaches. A graphical comparison of the NLO predictions and the large-N_C estimates has been made in figure 3 for different values of the renormalization scale μ.

JHEP02(2011)109

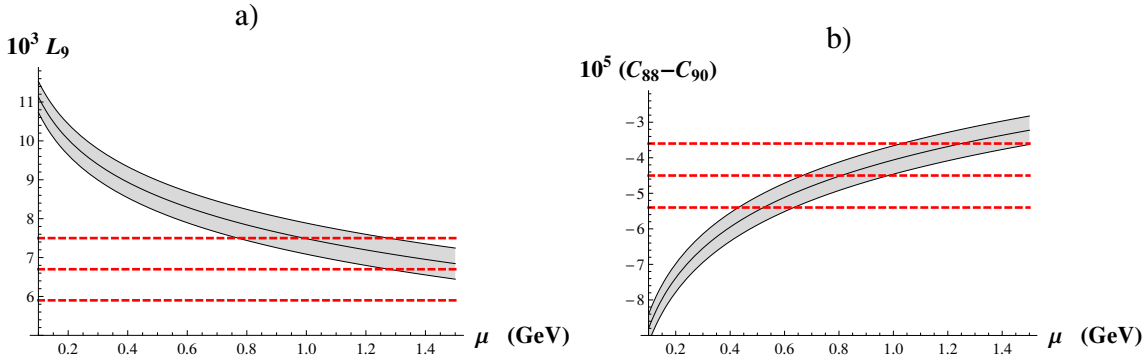

Figure 3. The RχT predictions (solid gray band) for the χPT $\mathcal{O}(p^4)$ low-energy constant $L_9(\mu)$ (a) and the $\mathcal{O}(p^6)$ combination $C_{88}(\mu) - C_{90}(\mu)$ (b) are compared to their large-N_C estimates (red dashed) for different values of the renormalization scale μ. The error of the large-N_C estimate is given by the naive saturation scale uncertainty from eq. (4.9).

It is appropriate to note the appreciable increase of $L_9(\mu_0)$ from the large-N_C prediction, for $\mu_0 = 770\,\text{MeV}$. In fact, the correction δ_{NLO} in eq. (3.6) gets a contribution from the $A\pi$ channel which is still comparable to that from the $\pi\pi$ one. This subleading contribution to $F_V G_V$, fixed through short-distance matching, increases the value of L_9 by $1 \cdot 10^{-3}$, a quite sizeable shift. For details see appendix E and ref. [52].

5 Conclusions

In this article we have completed the analysis of the VFF at NLO in $1/N_C$, initiated in ref. [18], where the general framework was established. We have considered operators with more than one resonance and have studied contributions from intermediate channels with resonances. We get a well-behaved VFF at high-energies, which goes to zero for $q^2 \to \infty$ [46, 47].

Imposing that each individual absorptive cut vanishes at short distances, one gets stringent constraints on the structure of the VFF, which led to a prediction of the relevant $\mathcal{O}(p^4)$ and $\mathcal{O}(p^6)$ χPT couplings up to NLO in $1/N_C$. The required inputs are the resonance masses M_V, M_A and M_S, and the pion decay constant F. As expected for such a well-known observable, the large-N_C prediction provides already an excellent estimate and the subleading corrections are relatively small. At the reference scale $\mu_0 = 770\,\text{MeV}$, we obtain

$$\begin{aligned} L_9(\mu_0) &= (7.9 \pm 0.4) \cdot 10^{-3}, \\ C_{88}(\mu_0) - C_{90}(\mu_0) &= (-4.6 \pm 0.4) \cdot 10^{-5}. \end{aligned} \tag{5.1}$$

As the matching of RχT with χPT is complete up to NLO in $1/N_C$, we fully control the running of the LECs up to that order and, e.g., we are able to predict $L_9(\mu)$ for any desired value of μ.

This result is in reasonable agreement with previous calculations [2–4, 37, 38, 45, 53, 54], see table 2, and shows once more the efficacy of RχT to describe low-energy QCD matrix elements, specially if they are dominated by resonances. It is important to remark

JHEP02(2011)109

	$10^3 \cdot L_9(\mu_0)$	$10^5 \cdot (C_{88}(\mu_0) - C_{90}(\mu_0))$
This work 1st	7.9 ± 0.4	-4.6 ± 0.4
This work 2nd	7.6 ± 0.6	-4.5 ± 0.5
Ref. [2–4]	6.9 ± 0.7	
Ref. [37, 38]	5.93 ± 0.43	-5.5 ± 0.5
Ref. [45]	7.04 ± 0.23	
Ref. [53] at $\mathcal{O}(p^4)$	6.54 ± 0.15	
Ref. [53] at $\mathcal{O}(p^6)$	5.50 ± 0.40	
Ref. [54]	6.3 ± 0.4	

Table 2. Comparison of our result with other determinations, being $\mu_0 = 770\,\text{MeV}$.

not only that the amplitude is dominated by tree-level exchanges but also the fact that the one-loop corrections are not large.

Our determination of $L_9(\mu_0)$ has a larger central value than the result obtained from an $\mathcal{O}(p^6)$ chiral fit to the VFF [37, 38] at low energies, and it is closer to the chiral fit determination at $\mathcal{O}(p^4)$ [2–4]. On the other hand, the ALEPH τ-data analysis performed in [45], which is also of $\mathcal{O}(p^6)$ but takes higher-energy data into account, yields a value of the order of $7 \cdot 10^{-3}$, much closer to our estimate.

In future works, we plan to study the pion scalar form-factor and the LECs $L_4(\mu)$ and $L_5(\mu)$, where the situation is much less clear since, in that case, one has contributions from broad resonance states like the $f_0(600)$.

Acknowledgments

We wish to thank Jaroslav Trnka for collaboration at an early stage of this project. This work has been supported by the Universidad CEU Cardenal Herrera, by the Generalitat Valenciana (Prometeo/2008/069), by the Generalitat de Catalunya (SGR 2005-00916), by the Spanish Government (FPA2007-60323, FPA2008-01430, the Juan de la Cierva program and Consolider-Ingenio 2010 CSD2007-00042, CPAN), and by the European Union (MRTN-CT-2006-035482, FLAVIAnet). J.J.S.C. wants to thank IFAE, where part of this work has been done.

A Dispersion relations and loop contribution

One may use a once-subtracted dispersion relation, derived from the identity

$$\frac{\mathcal{F}(s)}{s} = \frac{1}{2\pi i} \oint \mathrm{d}t \, \frac{\mathcal{F}(t)}{t\,(t-s)}\,, \tag{A.1}$$

where the integration is performed in the usual complex circuit [27]. The form-factor in the integrand can be written as

$$\frac{\mathcal{F}(t)}{t} = \frac{D(t)}{(M_V^2 - t)^2}\,, \tag{A.2}$$

JHEP02(2011)109

where $D(t)$ is an analytical function except for the unitarity logarithmic branch cut and the single pole of $\frac{\mathcal{F}(t)}{t}$ at $t=0$. One gets then

$$\frac{1}{s}\,\mathcal{F}(s)=\frac{1}{s}+\frac{1}{s}\,\mathcal{F}^{1\ell}(s)-\frac{\mathrm{Re}D'(M_V^2)}{M_V^2-s}+\frac{\mathrm{Re}D(M_V^2)}{(M_V^2-s)^2}\,, \tag{A.3}$$

where the $\frac{1}{s}$ term on the r.h.s. is given by the integration $\frac{1}{2\pi i}\int_{\theta=2\pi^-}^{\theta=0^+}\frac{dt}{t}\,\frac{\mathcal{F}(t)}{(t-s)}$, with $t=\epsilon\,e^{i\theta}$, around $t=0$ of the function $\frac{\mathcal{F}(t)}{t}\approx\frac{1}{t}+\mathcal{O}(t^0)$, and the different contributions of each two-meson absorptive cut are given by the dispersive integral,

$$\begin{aligned}\mathcal{F}^{1\ell}(s)|_{m_1,m_2}=\lim_{\epsilon\to 0}\Bigg[&\frac{s}{\pi}\int_0^{M_V^2-\epsilon}\mathrm{d}t\,\frac{\mathrm{Im}\mathcal{F}(t)|_{m_1,m_2}}{t\,(t-s)}+\frac{s}{\pi}\int_{M_V^2+\epsilon}^{\infty}\mathrm{d}t\,\frac{\mathrm{Im}\mathcal{F}(t)|_{m_1,m_2}}{t\,(t-s)}\\&-\frac{2s}{\pi\epsilon}\lim_{t\to M_V^2}\left\{(M_V^2-t)^2\,\frac{\mathrm{Im}\mathcal{F}(t)|_{m_1,m_2}}{t\,(t-s)}\right\}\Bigg]\,.\end{aligned} \tag{A.4}$$

Notice that if the threshold of the channel is above the resonance mass M_V, then this expression gets simplified into the form

$$\mathcal{F}^{1\ell}(s)|_{m_1,m_2}=\lim_{\epsilon\to 0}\frac{s}{\pi}\int_{(M_1+M_2)^2}^{\infty}\mathrm{d}t\,\frac{\mathrm{Im}\mathcal{F}(t)|_{m_1,m_2}}{t\,(t-s)}\,, \tag{A.5}$$

with M_1 (M_2) the mass of the m_1 (m_2) meson.

If we choose the on-shell mass scheme, without double poles in the perturbative expansion, we have then

$$\mathcal{F}(t)=1+\sum_{m_1,m_2}\mathcal{F}^{1\ell}(t)|_{m_1,m_2}-\frac{s\,\mathrm{Re}D'(M_V^2)}{M_V^2-t}\,, \tag{A.6}$$

where $\mathrm{Re}D'(M_V^2)$ can be identified with $-\frac{F_V^r G_V^r}{F^2}$ for a convenient renormalization scheme of this combination of vector couplings [26–28] (see appendix E for further details).

B The spectral functions $\mathrm{Im}\,\mathcal{F}(s)|_{m_1,m_2}$

In this appendix we show the explicit form of the the spectral functions of the different two-particle absorptive cuts. First we present the functions obtained directly from the Feynman diagrams before imposing any short-distance constraint, i.e., they are badly behaved at high energies.

$$\begin{aligned}\mathrm{Im}\,\mathcal{F}(s)|_{\pi\pi}=&\frac{F^2(M_V^2-s)+sF_VG_V}{64\pi F^6 s^2(s-M_V^2)}\Bigg\{2c_d^2\Bigg(M_S^4\log\left(1+\frac{s}{M_S^2}\right)(-12M_S^2-6s)+s^3\\&+12sM_S^4\Bigg)+G_V^2\Bigg(s^3-6M_V^2\,(M_V^2+2s)\left(\log\left(1+\frac{s}{M_V^2}\right)(2M_V^2+s)-2s\right)\Bigg)\Bigg\}\\&+\frac{s^2G_V\left(F^2(F_V+2G_V)(M_V^2-s)+2sF_VG_V^2\right)}{64\pi F^6(s-M_V^2)^2}+\frac{s}{64\pi F^2}\,,\end{aligned} \tag{B.1}$$

JHEP02(2011)109

$$
\begin{aligned}
\mathrm{Im}\,\mathcal{F}(s)|_{P\pi} = & \frac{\sqrt{2}c_d F_V \lambda_1^{\rm SP}\lambda_1^{\rm PV}}{32\pi F^4 s(s-M_V^2)}\Big\{3M_P^4(4M_S^2+s)-3M_P^2(2M_S^2+s)^2-M_P^6 \\
& -6M_S^2(M_S^2-M_P^2)(-M_P^2+2M_S^2+s)\log\Big(1+\frac{s-M_P^2}{M_S^2}\Big)+12sM_S^4+s^3\Big\} \\
& -\frac{F_V G_V \lambda_1^{\rm PV\,2}}{32\pi F^4 s(s-M_V^2)}\Big\{3M_P^2\left(12sM_V^2+4M_V^4+s^2\right)+6M_V^2\big(-3M_P^2(M_V^2+s) \\
& +M_P^4+5sM_V^2+2M_V^4+2s^2\big)\log\Big(1+\frac{s-M_P^2}{M_V^2}\Big)-3M_P^4(4M_V^2+s) \\
& +M_P^6-s(24sM_V^2+12M_V^4+s^2)-\frac{2s(s-M_P^2)^3}{s-M_V^2}\Big\}\,, \qquad \text{(B.2)}
\end{aligned}
$$

$$
\begin{aligned}
\mathrm{Im}\,\mathcal{F}(s)|_{A\pi} = & \frac{-G_V(s-M_A^2)^2}{32F^4\pi M_A^2 s(s-M_V^2)^2}\Big\{F_A\big((2\kappa+\sigma)M_A^4+4s(\kappa+\sigma)M_A^2+s^2\sigma\big)\big(s-M_V^2\big) \\
& -F_V\left(s-M_A^2\right)\big((2\kappa+\sigma)^2M_A^4+2s(\kappa^2+4\sigma\kappa+2\sigma^2)M_A^2+s^2\sigma^2\big)\Big\} \\
& -\frac{G_V}{32F^4\pi M_A^2 s(s-M_V^2)}\Big\{6\log\Big(1+\frac{s-M_A^2}{M_V^2}\Big)\Big(F_A(s-M_V^2)(M_A^2-M_V^2) \\
& \big(\kappa M_A^2+\sigma(M_V^2+s)\big)+F_V\big((M_A^2-s)(M_A^2-M_V^2)(M_V^2+s)\sigma^2+2\kappa M_A^2 \\
& (M_A^2-s)(M_A^2-M_V^2)\sigma+\kappa^2M_A^2\big(3M_A^4-5(M_V^2+s)M_A^2+(M_V^2+2s)(2M_V^2+s)\big)\big)\Big) \\
& M_V^2+(M_A^2-s)\Big(F_A(s-M_V^2)\big((3\kappa+\sigma)M_A^4+\big((3\sigma-6\kappa)M_V^2+s(3\kappa+4\sigma)\big)M_A^2 \\
& +\sigma(s^2-6M_V^4-3sM_V^2)\big)+F_V\big((M_A^2-s)\big(M_A^4+4sM_A^2-6M_V^4+s^2 \\
& +3(M_A^2-s)M_V^2\big)\sigma^2+6\kappa M_A^2(M_A^2-s)(M_A^2-2M_V^2+s)\sigma \\
& +\kappa^2M_A^2\big(7M_A^4-8(3M_V^2+s)M_A^2+12M_V^4+s^2+24sM_V^2\big)\big)\Big)\Big\} \\
& +\frac{\sqrt{2}c_d\lambda_1^{\rm SA}}{32F^4\pi s(s-M_V^2)}\Big\{6\log\Big(1+\frac{s-M_A^2}{M_S^2}\Big)\big(F_V\big(2\kappa M_S^4+(\kappa-\sigma)M_S^2 \\
& (s-M_A^2)+(\kappa+\sigma)M_A^2(s-M_A^2)\big)+F_A(M_A^2-M_S^2)(M_V^2-s)\big)M_S^2 \\
& +(M_A^2-s)\big(F_V\big(3\sigma(s-M_A^2)(M_A^2-2M_S^2+s) \\
& +\kappa(4sM_A^2-5M_A^4+12M_S^4+s^2)\big)+3F_A(M_A^2-2M_S^2+s)(M_V^2-s)\big)\Big\}\,, \qquad \text{(B.3)}
\end{aligned}
$$

where we have used the combination of couplings κ and σ,

$$
\kappa=-2\lambda_2^{\rm VA}+\lambda_3^{\rm VA}, \qquad \sigma=2\lambda_2^{\rm VA}-2\lambda_3^{\rm VA}+\lambda_4^{\rm VA}+2\lambda_5^{\rm VA}. \qquad \text{(B.4)}
$$

After considering the constraints explained in section 3,

$$
\begin{aligned}
F_V G_V &= F^2, & 3\,G_V^2+2\,c_d^2 &= F^2, \\
\lambda_1^{\rm PV} &= 0\,, & \kappa &= 0\,, \qquad \text{(B.5)} \\
\kappa+\sigma &= \frac{F_A}{F_V}\,, & \lambda_1^{\rm SA} &= -\frac{F_A\,G_V(M_A^2-4\,M_V^2)}{3\sqrt{2}M_A^2 c_d\,F_V}\,,
\end{aligned}
$$

JHEP02(2011)109

the imaginary part of each absorptive cut vanishes at short-distances and the following expressions are found,

$$\begin{aligned}
\mathrm{Im}\,\mathcal{F}(s)|_{\pi\pi} &= \frac{M_V^2}{32\pi F^4 s^2 (s-M_V^2)^2}\Bigg\{3M_S^4(F^2-3G_V^2)(M_V^2-s)\log\left(1+\frac{s}{M_S^2}\right)(2M_S^2+s) \\
&+G_V^2 M_V^2\Bigg(\log\left(1+\frac{s}{M_V^2}\right)(-6s^3-9s^2M_V^2+6M_V^6+9sM_V^4)+13s^3 \\
&-6s^2M_V^2-6sM_V^4\Bigg)+6sM_S^4(F^2-3G_V^2)(s-M_V^2)\Bigg\}\,, \qquad \text{(B.6)}\\
\mathrm{Im}\,\mathcal{F}(s)|_{P\pi} &= 0\,, \qquad \text{(B.7)}\\
\mathrm{Im}\,\mathcal{F}(s)|_{A\pi} &= \frac{F_A^2 G_V^2 (M_V^2-M_A^2)}{32\pi F^6 s M_A^2 (s-M_V^2)^2}\Bigg\{M_A^4\Bigg(2M_S^2(M_V^2-s)\Bigg(\log\left(1+\frac{s-M_A^2}{M_S^2}\right)-1\Bigg) \\
&+4sM_V^2-7M_V^4-3s^2\Bigg)+2M_A^2\Bigg(s^2M_V^2\Bigg(3\log\left(1+\frac{s-M_A^2}{M_V^2}\right)-2\Bigg) \\
&+M_S^4(s-M_V^2)\log\left(1+\frac{s-M_A^2}{M_S^2}\right)-M_S^2(s-M_V^2) \\
&\Bigg(s-4M_V^2\Bigg(\log\left(1+\frac{s-M_A^2}{M_S^2}\right)-1\Bigg)\Bigg)-3M_V^6\Bigg(\log\left(1+\frac{s-M_A^2}{M_V^2}\right)-1\Bigg)\Bigg) \\
&+M_V^2\Bigg(s^2M_V^2\Bigg(7-6\log\left(1+\frac{s-M_A^2}{M_V^2}\right)\Bigg)+8M_S^4(M_V^2-s)\log\left(1+\frac{s-M_A^2}{M_S^2}\right) \\
&+6M_V^6\log\left(1+\frac{s-M_A^2}{M_V^2}\right)+8sM_S^2(s-M_V^2)-6sM_V^4\Bigg)+2sM_A^6+M_A^8\Bigg\}\,. \qquad \text{(B.8)}
\end{aligned}$$

C Next-to-leading-order corrections $\mathcal{F}_{\rm NLO}(s)|_{m_1,m_2}$

In this appendix we show the explicit form of the NLO corrections generated by the considered two-particle absorptive cuts, eqs. (B.6), (B.7) and (B.8), which have been calculated by using the dispersive method discussed in appendix A. Below, we have summed up the $\delta_{\rm NLO}$ contribution to $\mathcal{F}^{1\ell}(s)$, as seen in eq. (3.6), being the different $\mathcal{F}_{\rm NLO}(s)|_{m_1m_2}$ well-behaved at high energies:

$$\begin{aligned}
\mathcal{F}_{\rm NLO}(s)|_{\pi\pi} &= \frac{M_V^2}{64\pi^2F^4 s(s-M_V^2)^2}\Bigg\{-12M_S^6(F^2-3G_V^2)(s-M_V^2)f(s,M_S^2) \\
&-6M_S^4(F^2-3G_V^2)(s-M_V^2)\Bigg(sf(s,M_S^2)+2\log\left(\frac{-s}{M_S^2}\right)-2\Bigg) \\
&+G_V^2M_V^2\Bigg(-6(3s^2M_V^2-3sM_V^4-2M_V^6+2s^3)f(s,M_V^2) \\
&+s^2\Bigg(-26\log\left(\frac{-s}{M_V^2}\right)+27\Bigg)+12M_V^4\Bigg(\log\left(\frac{-s}{M_V^2}\right)-1\Bigg) \\
&+3sM_V^2\Bigg(4\log\left(\frac{-s}{M_V^2}\right)-5\Bigg)\Bigg)+3sM_S^2(F^2-3G_V^2)(s-M_V^2)\Bigg\}\,, \qquad \text{(C.1)}
\end{aligned}$$

JHEP02(2011)109

$$\mathcal{F}_{\rm NLO}(s)|_{P\pi} = 0\,, \tag{C.2}$$

$$\begin{aligned}
\mathcal{F}_{\rm NLO}(s)|_{A\pi} = & -\frac{F_A^2 G_V^2 (M_A^2 - M_V^2)}{32\pi^2 F^6 s M_A^2 M_V^4 (s - M_V^2)^2} \Bigg\{ M_A^4 M_V^4 \Bigg(2sM_S^2 (M_V^2 - s) g(s, M_A^2, M_S^2) \\
& -6s^2 \log\left(1 - \frac{M_V^2}{M_A^2}\right) + \log\left(1 - \frac{s}{M_A^2}\right)\left(3s^2 + 2M_S^2(M_V^2 - s) + 7M_V^4 - 4sM_V^2\right) \Bigg) \\
& + sM_V^6 \Bigg(M_V^2 \Bigg(-6(s^2 - M_V^4) g(s, M_A^2, M_V^2) + 6M_V^2 \Bigg(\log\left(1 - \frac{s}{M_A^2}\right) - 1 \\
& + \log\left(\frac{M_A^2}{M_V^2}\right)\Bigg) + s\Bigg(-7\log\left(1 - \frac{s}{M_A^2}\right) - 6\log\left(\frac{M_A^2}{M_V^2}\right) + \log\left(1 - \frac{M_V^2}{M_A^2}\right) + 6\Bigg)\Bigg) \\
& + 8M_S^4 (M_V^2 - s) g(s, M_A^2, M_S^2) - 8M_S^2 (s - M_V^2)\Bigg(\log\left(1 - \frac{s}{M_A^2}\right) + \log\left(\frac{M_A^2}{M_S^2}\right) \\
& -1\Bigg)\Bigg) + M_A^2 M_V^4 \Bigg(M_V^2 \Bigg(6(s^3 - sM_V^4) g(s, M_A^2, M_V^2) + s^2 \Bigg(4\log\left(1 - \frac{s}{M_A^2}\right) \\
& + 2\log\left(1 - \frac{M_V^2}{M_A^2}\right) - 7\Bigg) - 6M_V^4 \log\left(1 - \frac{s}{M_A^2}\right) + 7sM_V^2 \Bigg) \\
& + 2sM_S^4 (s - M_V^2) g(s, M_A^2, M_S^2) \\
& + 2M_S^2 (s - M_V^2)\Bigg(4sM_V^2 g(s, M_A^2, M_S^2) + s\Bigg(\log\left(1 - \frac{s}{M_A^2}\right) + \log\left(\frac{M_A^2}{M_S^2}\right) - 1\Bigg) \\
& + 4M_V^2 \log\left(1 - \frac{s}{M_A^2}\right)\Bigg)\Bigg) + M_A^8 \Bigg(s^2 \log\left(1 - \frac{M_V^2}{M_A^2}\right) - M_V^4 \log\left(1 - \frac{s}{M_A^2}\right)\Bigg) \\
& + sM_A^6 M_V^2 \Bigg(M_V^2 \Bigg(-2\log\left(1 - \frac{s}{M_A^2}\right) - 1\Bigg) + 2s\log\left(1 - \frac{M_V^2}{M_A^2}\right) + s\Bigg)\Bigg\}\,,
\end{aligned} \tag{C.3}$$

where the functions $f(s, M^2)$ and $g(s, M_1^2, M_2^2)$ have been introduced for simplicity,

$$\begin{aligned}
f(s, M^2) &= \frac{1}{s}\left(\mathrm{Li}_2\left(1 + \frac{s}{M^2}\right) - \frac{\pi^2}{6}\right), \\
g(s, M_1^2, M_2^2) &= \frac{1}{s}\left(\mathrm{Li}_2\left(1 + \frac{s}{M_2^2} - \frac{M_1^2}{M_2^2}\right) - \mathrm{Li}_2\left(1 - \frac{M_1^2}{M_2^2}\right)\right).
\end{aligned} \tag{C.4}$$

D NLO contributions to $L_9(\mu)$ and $C_{88}(\mu) - C_{90}(\mu)$

In this appendix we give the full expressions of the NLO contributions to $L_9(\mu)$ and $C_{88}(\mu) - C_{90}(\mu)$, following the notation of eqs. (4.6) and (4.7), i.e., $\bar{\xi}^{(2)}_{m_1,m_2}$ and $\bar{\xi}^{(4)}_{m_1,m_2}$:

$$\bar{\xi}^{(2)}_{\pi\pi} = \frac{1}{768\pi^2 F^2}\left\{ F^2\left(6\log\left(\frac{M_S^2}{M_V^2}\right) - 11\right) + G_V^2\left(38 - 18\log\left(\frac{M_S^2}{M_V^2}\right)\right)\right\}, \tag{D.1}$$

$$\bar{\xi}^{(2)}_{P\pi} = 0\,, \tag{D.2}$$

JHEP02(2011)109

$$
\begin{aligned}
\bar{\xi}^{(2)}_{A\pi} = {} & \frac{F_A^2 G_V^2}{128\pi^2 F^4 M_A^2 M_V^8 (M_A^2 - M_S^2)} \Bigg\{ 2M_A^{10}(M_S^2 - M_A^2) \log\left(1 - \frac{M_V^2}{M_A^2}\right) \\
& -2M_A^8 M_V^2 (M_A^2 - M_S^2)\left(\log\left(1 - \frac{M_V^2}{M_A^2}\right) + 1\right) + M_A^6 M_V^4 (M_A^2 - M_S^2) \\
& \left(16\log\left(1-\frac{M_V^2}{M_A^2}\right)-3\right) + M_A^4 M_V^6 \left(M_S^2 \left(-2\log\left(\frac{M_A^2}{M_S^2}\right) + 16\log\left(1-\frac{M_V^2}{M_A^2}\right) - 11\right)\right. \\
& \left. + M_A^2 \left(11 - 16\log\left(1-\frac{M_V^2}{M_A^2}\right)\right)\right) + M_A^2 M_V^8 \left(M_S^2 \left(10\log\left(\frac{M_A^2}{M_S^2}\right) - 12\log\left(\frac{M_A^2}{M_V^2}\right)\right.\right. \\
& \left. -2\log\left(1 - \frac{M_V^2}{M_A^2}\right) + 11\right) + M_A^2 \left(12\log\left(\frac{M_A^2}{M_V^2}\right) + 2\log\left(1 - \frac{M_V^2}{M_A^2}\right) - 11\right)\Bigg) \\
& + M_V^{10} \left(M_A^2 \left(-6\log\left(\frac{M_A^2}{M_V^2}\right) + 2\log\left(1 - \frac{M_V^2}{M_A^2}\right) + 5\right)\right. \\
& \left. - M_S^2 \left(8\log\left(\frac{M_A^2}{M_S^2}\right) - 6\log\left(\frac{M_A^2}{M_V^2}\right) + 2\log\left(1 - \frac{M_V^2}{M_A^2}\right) + 5\right)\right)\Bigg\}, \qquad \text{(D.3)}
\end{aligned}
$$

$$
\begin{aligned}
\bar{\xi}^{(4)}_{\pi\pi} = {} & \frac{1}{3072\pi^2 M_V^2} \left\{ 2F^2 \left(11 - 6\log\left(\frac{M_S^2}{M_V^2}\right)\right) + G_V^2 \left(36\log\left(\frac{M_S^2}{M_V^2}\right) - 11\right)\right\} \\
& + \frac{(F^2 - 3G_V^2)}{3072\pi^2 M_S^2} \left\{ 12\log\left(\frac{M_S^2}{M_V^2}\right) - 19\right\}, \qquad \text{(D.4)}
\end{aligned}
$$

$$
\bar{\xi}^{(4)}_{P\pi} = 0\,, \qquad \text{(D.5)}
$$

$$
\begin{aligned}
\bar{\xi}^{(4)}_{A\pi} = {} & \frac{-F_A^2 G_V^2}{384\pi^2 F^2 M_A^2 M_V^{10} (M_A^2 - M_S^2)^2 (M_A^2 - M_V^2)} \Bigg\{ -6M_A^{10} M_V^2 (M_A^2 - M_S^2)^2 \\
& + 8M_V^{14} \left(M_S^2 \left(\log\left(\frac{M_A^2}{M_S^2}\right) + 1\right) - M_A^2\right) - M_V^{12} \left(2M_A^2 M_S^2 \left(3\log\left(\frac{M_A^2}{M_S^2}\right) + 6\log\left(\frac{M_A^2}{M_V^2}\right)\right.\right. \\
& \left. -6\log\left(1-\frac{M_V^2}{M_A^2}\right) + 4\right) + M_S^4 \left(12\log\left(\frac{M_A^2}{M_S^2}\right) - 6\log\left(\frac{M_A^2}{M_V^2}\right) + 6\log\left(1-\frac{M_V^2}{M_A^2}\right) + 5\right) \\
& \left. + M_A^4 \left(-6\log\left(\frac{M_A^2}{M_V^2}\right) + 6\log\left(1 - \frac{M_V^2}{M_A^2}\right) - 13\right)\right) - 3M_A^2 M_V^{10} \left(M_A^2 M_S^2 \right. \\
& \left(5\log\left(\frac{M_A^2}{M_S^2}\right) - 12\log\left(\frac{M_A^2}{M_V^2}\right) + 22\right) + M_S^4 \left(-9\log\left(\frac{M_A^2}{M_S^2}\right) + 6\log\left(\frac{M_A^2}{M_V^2}\right) - 13\right) \\
& \left. + M_A^4 \left(6\log\left(\frac{M_A^2}{M_V^2}\right) - 9\right)\right) + 2M_A^4 M_V^8 \left(M_A^2 M_S^2 \left(8\log\left(\frac{M_A^2}{M_S^2}\right) - 18\log\left(\frac{M_A^2}{M_V^2}\right)\right.\right. \\
& \left. -54\log\left(1-\frac{M_V^2}{M_A^2}\right) + 71\right) + 9M_S^4 \left(\log\left(\frac{M_A^2}{M_V^2}\right) - \log\left(\frac{M_A^2}{M_S^2}\right) + 3\log\left(1-\frac{M_V^2}{M_A^2}\right) - 4\right) \\
& \left. + M_A^4 \left(9\log\left(\frac{M_A^2}{M_V^2}\right) + 27\log\left(1 - \frac{M_V^2}{M_A^2}\right) - 35\right)\right) - M_A^6 M_V^6 (M_A^2 - M_S^2) \\
& \left(M_S^2 \left(3\log\left(\frac{M_A^2}{M_S^2}\right) - 96\log\left(1-\frac{M_V^2}{M_A^2}\right) + 47\right) + M_A^2 \left(96\log\left(1-\frac{M_V^2}{M_A^2}\right) - 47\right)\right) \\
& + 3M_A^8 M_V^4 (M_A^2 - M_S^2)^2 \left(18\log\left(1-\frac{M_V^2}{M_A^2}\right) - 1\right) - 6M_A^{12} (M_A^2 - M_S^2)^2 \log\left(1-\frac{M_V^2}{M_A^2}\right)\Bigg\}. \qquad \text{(D.6)}
\end{aligned}
$$

JHEP02(2011)109

E Description in terms of Feynman diagrams

The subleading corrections can be calculated by means of dispersive relations. Once the NLO absorptive parts of $\mathcal{F}_{R\chi T}(s)$ are known, one can reconstruct the full form factor up to appropriate subtraction terms. Alternatively, we can compute and separate the tree-level and one-loop amplitudes in the form

$$\mathcal{F}_{R\chi T}(s) = 1 + \frac{F_V G_V}{F^2}\frac{s}{M_V^2 - s} + \frac{2\widetilde{L}_9}{F^2}\, s + \sum_{m_1,m_2} \mathcal{F}(s)|_{m_1,m_2}\,, \tag{E.1}$$

where the one-loop diagrams $\mathcal{F}(s)|_{m_1,m_2}$ can be rewritten by means of a once-subtracted dispersion relation in the form

$$\sum_{m_1,m_2} \mathcal{F}(s)|_{m_1,m_2} = \sum_{m_1,m_2} \mathcal{F}^{1\ell}(s)|_{m_1,m_2} + \frac{2\hat{\delta}_2}{F^2}\, s + \hat{\delta}_0 \frac{s}{M_V^2 - s} + \hat{\delta}_{-2}\frac{s}{(M_V^2 - s)^2}\,. \tag{E.2}$$

The finite part of the loops is contained in the once-subtracted dispersive functions $\mathcal{F}^{1\ell}(s)|_{m_1,m_2}$, fully determined by the imaginary part of $\mathrm{Im}\mathcal{F}(s)|_{m_1,m_2}$ through eq. (A.4). The real parameters $\hat{\delta}_{-2,0,2}$ contain the ultraviolet divergences of the loops, being $\hat{\delta}_0$ and $\hat{\delta}_{-2}$ the real part of the pole residues. The local RχT coupling $\widetilde{L}_9$ renormalizes $\hat{\delta}_2$, the combination $F_V G_V$ cancels the divergences in $\hat{\delta}_0$ and a convenient shift of the mass, $M_V^{(B)\,2} = M_V^2 + \delta M_V^2$ removes the divergent part of $\hat{\delta}_{-2}$. Indeed, we will work in the on-shell scheme and the counterterm δM_V^2 will be chosen to completely kill $\hat{\delta}_{-2}$.

In order to finish the short-distance matching we just need to take into account that the once-subtracted loop contribution behaves at short distances like

$$\sum_{m_1,m_2} \mathcal{F}^{1\ell}(s)|_{m_1,m_2} \quad \stackrel{s\to\infty}{\longrightarrow} \quad \delta_0 + \mathcal{O}(s^{-1})\,, \tag{E.3}$$

with δ_0 a constant number (denoted before in the text as $\delta_{_{NLO}}$). This leads to the VFF high-energy constraints

$$\begin{aligned} \frac{F_V G_V}{F^2} + \hat{\delta}_0 &= 1 + \delta_0\,, \\ \widetilde{L}_9 + \hat{\delta}_2 &= 0\,. \end{aligned} \tag{E.4}$$

Hence, the VFF finally takes the well-behaved structure (3.5) employed in the article,

$$\begin{aligned} \mathcal{F}(s) &= 1 + \big(1 + \delta_0\big)\frac{s}{M_V^2 - s} + \sum_{m_1,m_2} \mathcal{F}^{1\ell}(s)|_{m_1,m_2} \\ &= \frac{M_V^2}{M_V^2 - s} + \mathcal{F}_{\rm NLO}(s)\,. \end{aligned} \tag{E.5}$$

Notice that no real double pole term $\hat{\delta}_{-2}$ remains in our perturbative NLO expression as we have chosen the on-shell mass scheme.

JHEP02(2011)109

References

[1] S. Weinberg, *Phenomenological Lagrangians*, *Physica* **A 96** (1979) 327 [SPIRES].

[2] J. Gasser and H. Leutwyler, *Chiral perturbation theory to one loop*, *Ann. Phys.* **158** (1984) 142 [SPIRES].

[3] J. Gasser and H. Leutwyler, *Chiral perturbation theory: expansions in the mass of the strange quark*, *Nucl. Phys.* **B 250** (1985) 465 [SPIRES].

[4] J. Gasser and H. Leutwyler, *Low-energy expansion of meson form-factors*, *Nucl. Phys.* **B 250** (1985) 517 [SPIRES].

[5] J. Bijnens, G. Colangelo and G. Ecker, *The mesonic chiral Lagrangian of order p^6*, *JHEP* **02** (1999) 020 [hep-ph/9902437] [SPIRES].

[6] J. Bijnens, G. Colangelo and G. Ecker, *Renormalization of chiral perturbation theory to order p^6*, *Annals Phys.* **280** (2000) 100 [hep-ph/9907333] [SPIRES].

[7] G. 't Hooft, *A planar diagram theory for strong interactions*, *Nucl. Phys.* **B 72** (1974) 461 [SPIRES].

[8] G. 't Hooft, *A two-dimensional model for mesons*, *Nucl. Phys.* **B 75** (1974) 461 [SPIRES].

[9] E. Witten, *Baryons in the $1/N$ expansion*, *Nucl. Phys.* **B 160** (1979) 57 [SPIRES].

[10] M. Knecht and E. de Rafael, *Patterns of spontaneous chiral symmetry breaking in the large-N_c limit of QCD-like theories*, *Phys. Lett.* **B 424** (1998) 335 [hep-ph/9712457] [SPIRES].

[11] S. Peris, M. Perrottet and E. de Rafael, *Matching long and short distances in large-N_c QCD*, *JHEP* **05** (1998) 011 [hep-ph/9805442] [SPIRES].

[12] M. Golterman and S. Peris, *Large-N_c QCD meets Regge theory: the example of spin-one two-point functions*, *JHEP* **01** (2001) 028 [hep-ph/0101098] [SPIRES].

[13] A. Pich, *Low-energy constants from resonance chiral theory*, PoS(CONFINEMENT8)026 [arXiv:0812.2631] [SPIRES].

[14] G. Ecker, J. Gasser, A. Pich and E. de Rafael, *The role of resonances in chiral perturbation theory*, *Nucl. Phys.* **B 321** (1989) 311 [SPIRES].

[15] G. Ecker, J. Gasser, H. Leutwyler, A. Pich and E. de Rafael, *Chiral Lagrangians for massive spin 1 fields*, *Phys. Lett.* **B 223** (1989) 425 [SPIRES].

[16] V. Cirigliano et al., *Towards a consistent estimate of the chiral low-energy constants*, *Nucl. Phys.* **B 753** (2006) 139 [hep-ph/0603205] [SPIRES].

[17] O. Catà and S. Peris, *An example of resonance saturation at one loop*, *Phys. Rev.* **D 65** (2002) 056014 [hep-ph/0107062] [SPIRES].

[18] I. Rosell, J.J. Sanz-Cillero and A. Pich, *Quantum loops in the resonance chiral theory: the vector form factor*, *JHEP* **08** (2004) 042 [hep-ph/0407240] [SPIRES].

[19] I. Rosell, P. Ruiz-Femenia and J. Portoles, *One-loop renormalization of resonance chiral theory: scalar and pseudoscalar resonances*, *JHEP* **12** (2005) 020 [hep-ph/0510041] [SPIRES].

[20] J.J. Sanz-Cillero, *On the structure of two-point Green functions at next-to-leading order in $1/N_C$*, *Phys. Lett.* **B 649** (2007) 180 [hep-ph/0702217] [SPIRES].

JHEP02(2011)109

[21] L.Y. Xiao and J.J. Sanz-Cillero, *Renormalizable sectors in resonance chiral theory: $S \to \pi\pi$ decay amplitude*, *Phys. Lett.* **B 659** (2008) 452 [arXiv:0705.3899] [SPIRES].

[22] J. Portoles, I. Rosell and P. Ruiz-Femenia, *Vanishing chiral couplings in the large-N_c resonance theory*, *Phys. Rev.* **D 75** (2007) 114011 [hep-ph/0611375] [SPIRES].

[23] I. Rosell, P. Ruiz-Femenia and J.J. Sanz-Cillero, *Resonance saturation of the chiral couplings at NLO in $1/N_C$*, *Phys. Rev.* **D 79** (2009) 076009 [arXiv:0903.2440] [SPIRES].

[24] I. Rosell, *Quantum corrections in the resonance chiral theory*, hep-ph/0701248 [SPIRES].

[25] K. Kampf, J. Novotny and J. Trnka, *Renormalization and additional degrees of freedom within the chiral effective theory for spin-1 resonances*, *Phys. Rev.* **D 81** (2010) 116004 [arXiv:0912.5289] [SPIRES].

[26] I. Rosell, J.J. Sanz-Cillero and A. Pich, *Towards a determination of the chiral couplings at NLO in $1/N_C$: $L_8^r(\mu)$ and $C_{38}^r(\mu)$*, *JHEP* **01** (2007) 039 [hep-ph/0610290] [SPIRES].

[27] A. Pich, I. Rosell and J.J. Sanz-Cillero, *Form-factors and current correlators: chiral couplings $L_{10}(\mu)$ and $C_{87}(\mu)$ at NLO in $1/N_C$*, *JHEP* **07** (2008) 014 [arXiv:0803.1567] [SPIRES].

[28] J.J. Sanz-Cillero and J. Trnka, *High energy constraints in the octet SS-PP correlator and resonance saturation at NLO in $1/N_C$*, *Phys. Rev.* **D 81** (2010) 056005 [arXiv:0912.0495] [SPIRES].

[29] J. Bijnens, E. Gamiz, E. Lipartia and J. Prades, *QCD short-distance constraints and hadronic approximations*, *JHEP* **04** (2003) 055 [hep-ph/0304222] [SPIRES].

[30] S. Peris, *Large-N_C QCD and Pade approximant theory*, *Phys. Rev.* **D 74** (2006) 054013 [hep-ph/0603190] [SPIRES].

[31] P. Masjuan and S. Peris, *A rational approach to resonance saturation in large-N_C QCD*, *JHEP* **05** (2007) 040 [arXiv:0704.1247] [SPIRES].

[32] M. Golterman, S. Peris, B. Phily and E. De Rafael, *Testing an approximation to large-N_C QCD with a toy model*, *JHEP* **01** (2002) 024 [hep-ph/0112042] [SPIRES].

[33] J.J. Sanz-Cillero, *Spin-1 correlators at large-N_C: matching OPE and resonance theory up to $\mathcal{O}(\alpha_s)$*, *Nucl. Phys.* **B 732** (2006) 136 [hep-ph/0507186] [SPIRES].

[34] M. Golterman and S. Peris, *On the relation between low-energy constants and resonance saturation*, *Phys. Rev.* **D 74** (2006) 096002 [hep-ph/0607152] [SPIRES].

[35] S. Weinberg, *Precise relations between the spectra of vector and axial vector mesons*, *Phys. Rev. Lett.* **18** (1967) 507 [SPIRES].

[36] M.A. Shifman, A.I. Vainshtein and V.I. Zakharov, *QCD and resonance physics. Sum rules*, *Nucl. Phys.* **B 147** (1979) 385 [SPIRES].

[37] J. Bijnens, G. Colangelo and P. Talavera, *The vector and scalar form factors of the pion to two loops*, *JHEP* **05** (1998) 014 [hep-ph/9805389] [SPIRES].

[38] J. Bijnens and P. Talavera, *Pion and kaon electromagnetic form factors*, *JHEP* **03** (2002) 046 [hep-ph/0203049] [SPIRES].

[39] F. Guerrero and A. Pich, *Effective field theory description of the pion form factor*, *Phys. Lett.* **B 412** (1997) 382 [hep-ph/9707347] [SPIRES].

[40] D. Gomez Dumm, A. Pich and J. Portoles, *The hadronic off-shell width of meson resonances*, *Phys. Rev.* **D 62** (2000) 054014 [hep-ph/0003320] [SPIRES].

JHEP02(2011)109

[41] D. Gomez Dumm, A. Pich and J. Portoles, $\tau \to (3\pi)\nu_\tau$ *decays in the resonance effective theory*, *Phys. Rev.* **D 69** (2004) 073002 [hep-ph/0312183] [SPIRES].

[42] J.A. Oller, E. Oset and J.E. Palomar, *Pion and kaon vector form factors*, *Phys. Rev.* **D 63** (2001) 114009 [hep-ph/0011096] [SPIRES].

[43] A. Pich and J. Portoles, *The vector form factor of the pion from unitarity and analyticity: a model-independent approach*, *Phys. Rev.* **D 63** (2001) 093005 [hep-ph/0101194] [SPIRES].

[44] J.J. Sanz-Cillero, *Renormalization group equations in resonance chiral theory*, *Phys. Lett.* **B 681** (2009) 100 [arXiv:0905.3676] [SPIRES].

[45] J.J. Sanz-Cillero and A. Pich, *Rho meson properties in the chiral theory framework*, *Eur. Phys. J.* **C 27** (2003) 587 [hep-ph/0208199] [SPIRES].

[46] G.P. Lepage and S.J. Brodsky, *Exclusive processes in quantum chromodynamics: evolution equations for hadronic wave functions and the form-factors of mesons*, *Phys. Lett.* **B 87** (1979) 359 [SPIRES].

[47] G.P. Lepage and S.J. Brodsky, *Exclusive processes in perturbative quantum chromodynamics*, *Phys. Rev.* **D 22** (1980) 2157 [SPIRES].

[48] Z.H. Guo, J.J. Sanz Cillero and H.Q. Zheng, *Partial waves and large-N_C resonance sum rules*, *JHEP* **06** (2007) 030 [hep-ph/0701232] [SPIRES].

[49] Z.-H. Guo and P. Roig, *One meson radiative tau decays*, *Phys. Rev.* **D 82** (2010) 113016 [arXiv:1009.2542] [SPIRES].

[50] Particle Data Group collaboration, K. Nakamura et al., *Review of particle physics*, *J. Phys.* **G 37** (2010) 075021 [SPIRES].

[51] V. Mateu and J. Portoles, *Form factors in radiative pion decay*, *Eur. Phys. J.* **C 52** (2007) 325 [arXiv:0706.1039] [SPIRES].

[52] J.J. Sanz-Cillero, *One loop predictions for the pion VFF in resonance chiral theory*, *AIP Conf. Proc.* **1317** (2011) 116 [arXiv:1009.6012] [SPIRES].

[53] M. Gonzalez-Alonso, A. Pich and J. Prades, *Determination of the chiral couplings L_{10} and C_{87} from semileptonic tau decays*, *Phys. Rev.* **D 78** (2008) 116012 [arXiv:0810.0760] [SPIRES].

[54] P. Masjuan, S. Peris and J.J. Sanz-Cillero, *Vector meson dominance as a first step in a systematic approximation: the pion vector form factor*, *Phys. Rev.* **D 78** (2008) 074028 [arXiv:0807.4893] [SPIRES].

JHEP02(2011)109